# Calcium Salts of Biobased Anionic Surfactant Result in Hydrophilic, Air-Stable Bilayers by Distorted Hydrogen-Bond Networks

*Taichi Habe[1], Tadashi Sugahara[2], Hiroko Endo[3], Kana Tsumura[2], Atsushi Miyazaki[2], Kenta Motobayashi[4], Andreas Stöcklin[5], Shigeto Inoue*[1,6], Takaya Sakai*[7], Motomu Tanaka*[5,8]*

[1]Analytical Science Research Laboratories, Kao Corporation, 3-25-40, Minato, Wakayamashi, Wakayama 640-8580, Japan

[2]Biological Material Science Research Laboratories, Kao Corporation, 1334, Minato, Wakayama-shi, Wakayama 640-8580, Japan

[3]Biological material Science Research Laboratories, Kao Corporation, 2-1-3, Bunka, Sumida -ku, Tokyo 131-8501, Japan

[4]Program of Applied Physics, Department of Engineering, Nagoya Institute of Technology, Nagoya 466-8555, Japan

[5]Physical Chemistry of Biosystems, Institute of Physical Chemistry, Heidelberg University, 69120 Heidelberg, Germany

[6]Analytical Science Research Laboratories, Kao Corporation, 3-25-40, Minato, Wakayama-shi, Wakayama 640-8580, Japan; Phone: +1 513 658 8832; E-mail: shigeto.inoue@kao.com

[7]Core Technology Research Center, R&D, Kao Corporation, 2-1-3, Bunka, Sumida-ku, Tokyo 131-8501, Japan; Phone: +81 -80-3394-3646; E-mail: sakai.takaya@kao.com

[8]Center for Integrative Medicine and Physics, Kyoto University, Kyoto 606-8502, Japan; Phone: +49 6221 544916; E-mail: tanaka@uni-heidelberg.de

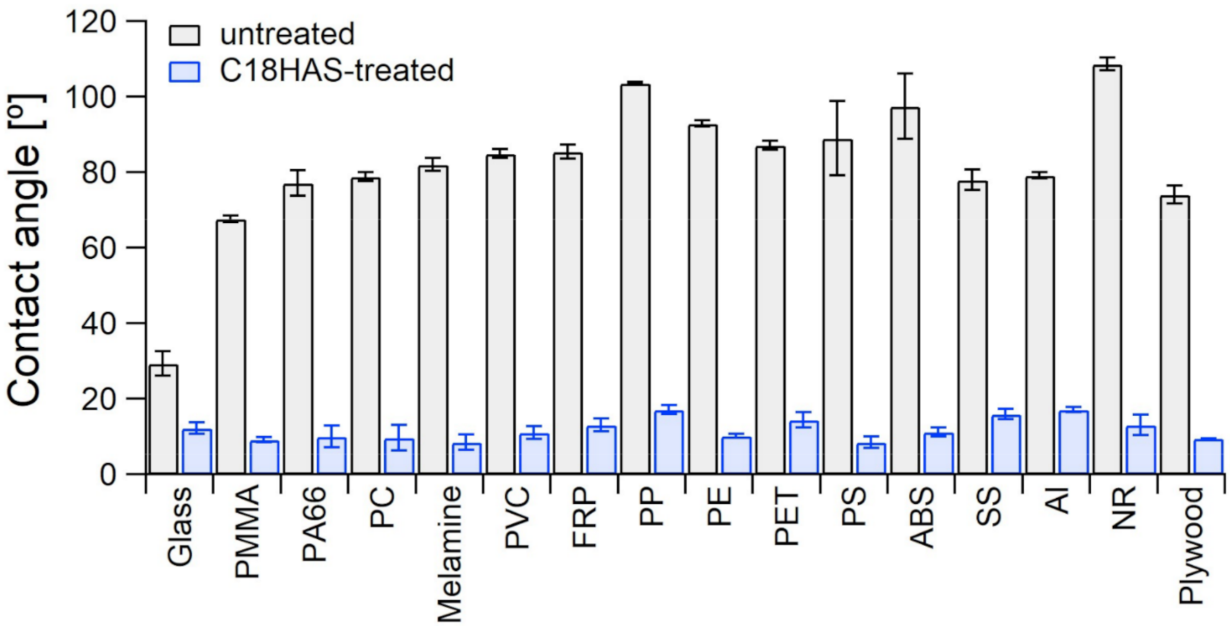


Figure S1. Water contact angle data before (grey) and after (blue) C18HAS treatment following the protocol described in Ref. 36. Each data point consists of mean ± standard deviations from *N* = 3 independent measurements. PMMA; polymethyl methacrylate, PA66; polyamide 66, PC; polycarbonate, PVC; polyvinyl chloride, FRP; fiber-reinforced plastic, PP; polypropylene, PE; polyethylene, PET; poly(ethylene terephthalate), PS; polystyrene, ABS; acrylonitrile-butadiene-styrene, SS; stainless steel, Al; aluminum, NR; natural rubber.

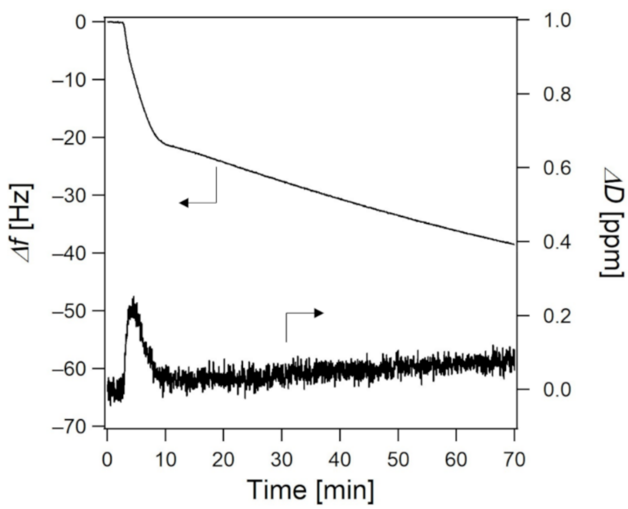


Figure S2. Changes in frequency (Δ*f*) and dissipation (Δ*D*) as measured by QCM-D during the adsorption of C18HAS vesicles onto $SiO_2$ sensor. A continuous drift of Δ*f* suggests the formation of multilayers.

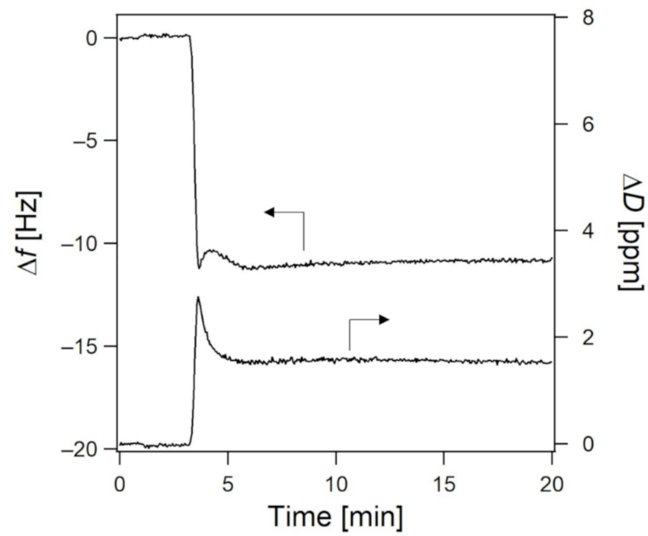


Figure S3. Changes in frequency ($\Delta f$) and dissipation ($\Delta D$) as measured by QCM-D during the adsorption of DODAB vesicles onto $SiO_2$ sensor. The small shift in resonant frequency, $\Delta f = -11$ Hz, suggests the formation of a thin, interdigitated membrane.

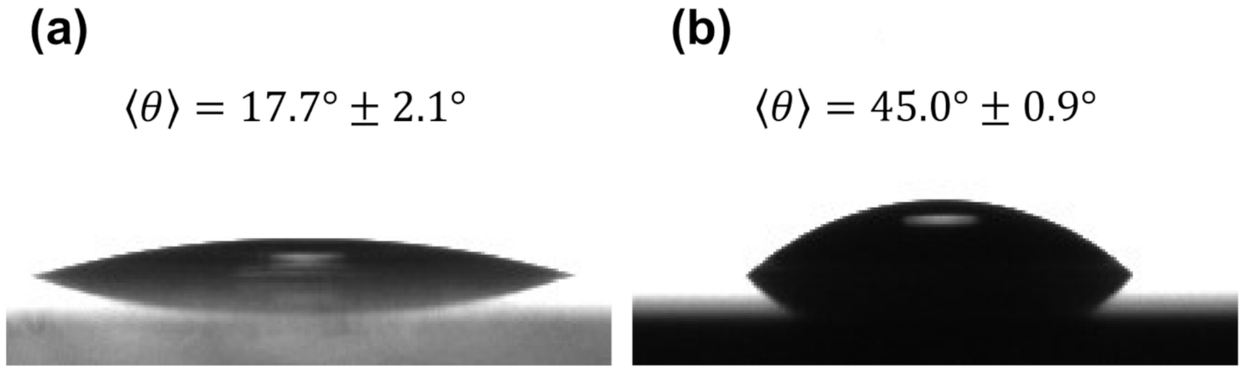


Figure S4. Water droplets on C18HAS-treated gold surface before (a) and after (b) exposure to vacuum ($p < 1.0 \times 10^{-5}$ Pa).

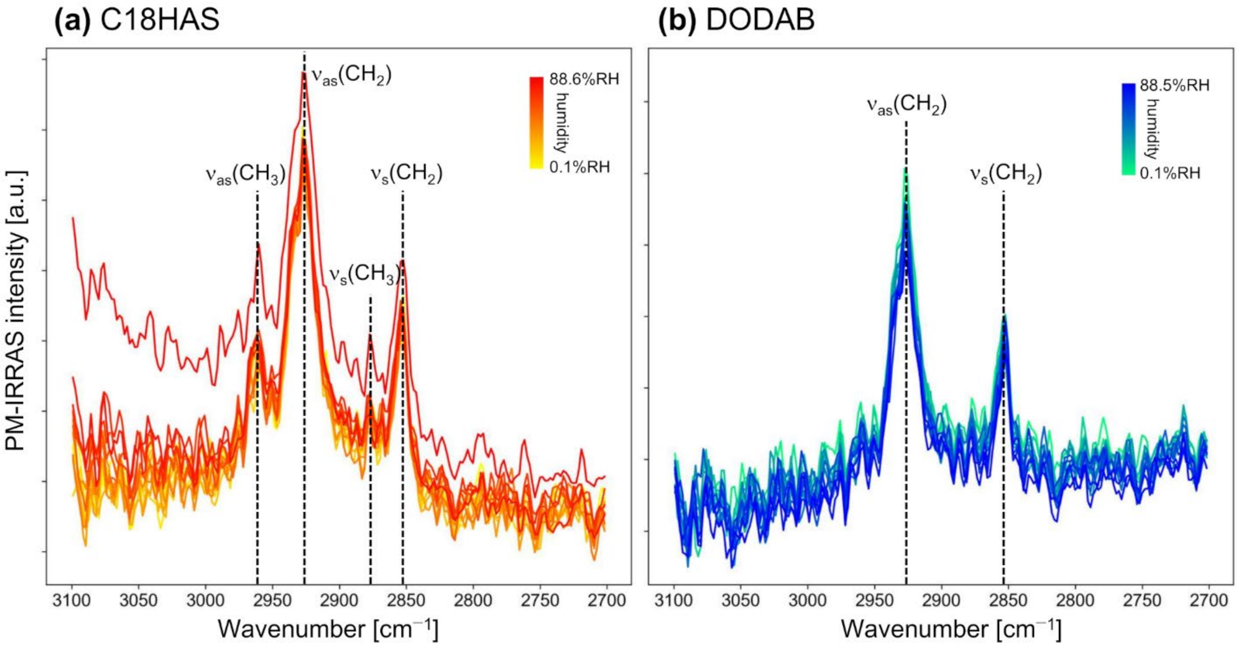


Figure S5. PM-IRRAS spectra in the CH region for (a) C18HAS and (b) DODAB adsorbates on gold substrate exposed to different relative humidities.

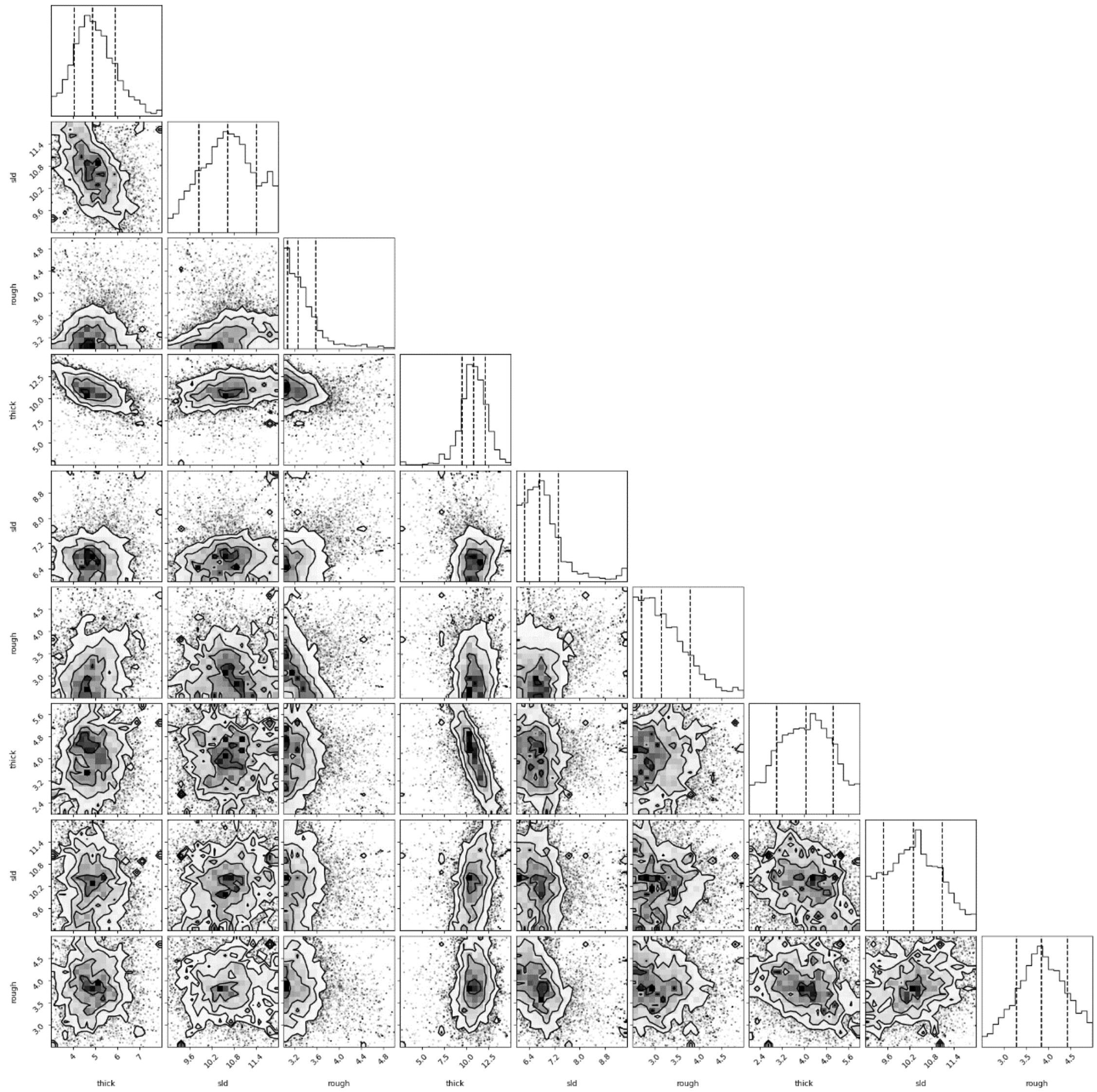


Figure S6. MCMC steps corner for the best fit of XRR data of single C18HAS layer measured at *RH* = 93 %. For each *RH*, 10 MCMC fits were performed, and the fit with the lowest $\chi^2$ was used. Motofit refnx 0.1.16 was used with the settings: 200 steps, 200 walkers (A.R.J. Nelson and S.W. Prescot, *J. Appl. Crystallography*, 52, 193 (2019)).

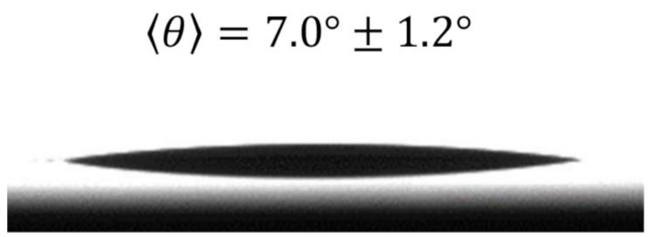


Figure S7. Water droplets on $SiO_2$ substrate pretreated with suspension of C18HAS for 120 min. The observed contact angle is $\langle\theta\rangle = 7.0° \pm 1.2°$.

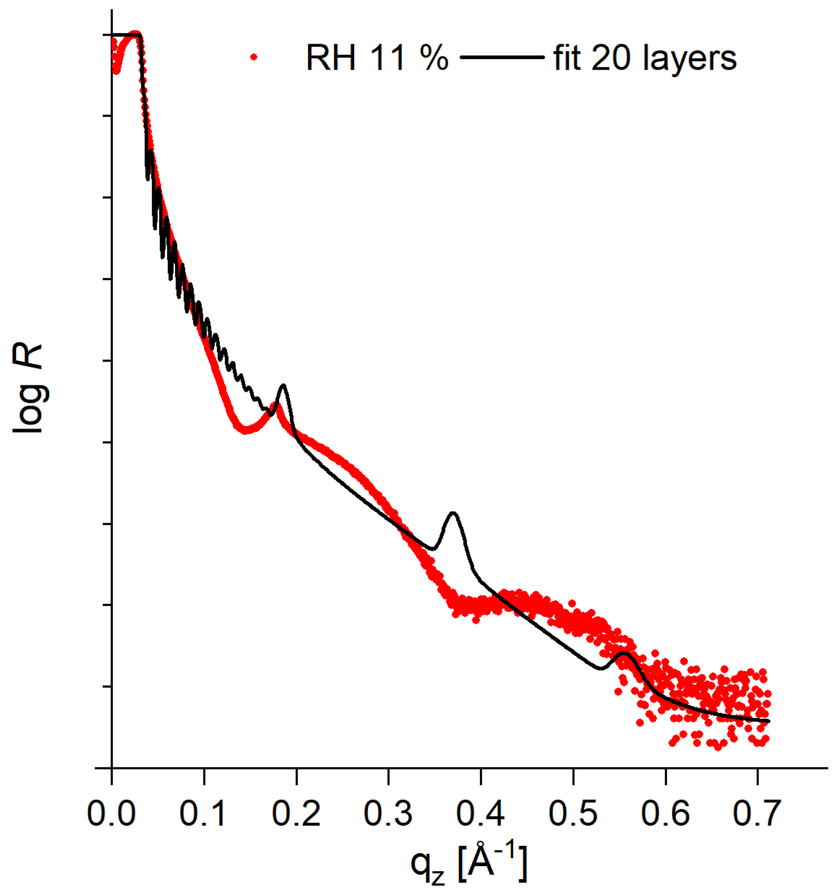


Figure S8. Fitting curve (black) assuming the stacks of uniform multilayer stacks (20 × bilayers). The fit resulted in many Kiessig fringes and was not able to reproduce the experimental data, indicating the necessity of model improvement.

Table S1. Layer parameters of C18HAS multilayers obtained by XRR. The best fit results could be obtained by assuming that multilayers consist of (i) 2 bilayers coating the entire surface and (ii) 11 – 13 additional bilayer patches coating 15% of the surface. To reduce the number of fitting parameters, two head layers were parameterized identically.

| *RH* = 11 % | | | |
|---|---|---|---|
| | $d$ [Å] | *SLD* [Å$^{-2}$] | $\sigma$ [Å] |
| Head (2 bilayers) | 3.72 ± 0.16 | 10.22 ± 0.46 | 3.76 ± 0.26 |
| Chain (2 bilayers) | 4.25 ± 0.65 | 7.48 ± 0.87 | 3.76 ± 0.26 |
| Head (patches) | 4.31 ± 0.25 | 10.41 ± 0.30 | 3.37 ± 0.29 |
| Chain (patches) | 19.40 ± 0.43 | 8.52 ± 0.41 | 3.37 ± 0.29 |
| *RH* = 53 % | | | |
| | $d$ [Å] | *SLD* [Å$^{-2}$] | $\sigma$ [Å] |
| Head (2 bilayers) | 3.70 ± 0.14 | 10.49 ± 0.30 | 3.52 ± 0.22 |
| Chain (2 bilayers) | 5.06 ± 0.69 | 7.57 ± 0.85 | 3.52 ± 0.22 |
| Head (patches) | 4.43 ± 0.30 | 10.43 ± 0.30 | 3.36 ± 0.27 |
| Chain (patches) | 21.09 ± 0.43 | 8.15 ± 0.52 | 3.36 ± 0.27 |
| *RH* = 84 % | | | |
| | $d$ [Å] | *SLD* [Å$^{-2}$] | $\sigma$ [Å] |
| Head (2 bilayers) | 3.71 ± 0.15 | 10.11 ± 0.42 | 3.15 ± 0.16 |
| Chain (2 bilayers) | 17.11 ± 0.43 | 6.50 ± 0.48 | 3.15 ± 0.16 |
| Head (patches) | 4.44 ± 0.31 | 10.33 ± 0.27 | 3.51 ± 0.33 |
| Chain (patches) | 25.83 ± 0.63 | 8.46 ± 0.43 | 3.51 ± 0.33 |

| $RH = 93$ % | | | |
|---|---|---|---|
| | $d$ [Å] | $SLD$ [Å$^{-2}$] | $\sigma$ [Å] |
| Head (2 bilayers) | 3.93 ± 0.25 | 10.04 ± 0.39 | 3.16 ± 0.15 |
| Chain (2 bilayers) | 17.84 ± 0.46 | 6.74 ± 0.53 | 3.16 ± 0.15 |
| Head (patches) | 4.39 ± 0.26 | 10.37 ± 0.34 | 3.63 ± 0.31 |
| Chain (patches) | 27.44 ± 0.33 | 8.07 ± 0.75 | 3.63 ± 0.31 |